



Crystal growth and dissolution processes at the calcite–water interface in the presence of zinc ions

Sawsan J. Freij^{a,b,*}, Athanasios Godelitsas^{a,c}, Andrew Putnis^a

^a*Institute für Mineralogie, Westfälische Wilhelms-Universität Münster, Correnstrasse 23, D-48139 Münster, Germany*

^b*Centre for Fuels and Energy, Curtin University of Technology, GPO Box U1987, Perth, WA 6845, Australia*

^c*Department of Mineralogy and Petrology, University of Athens, 15784 Ano Ilissia, Greece*

Received 12 May 2004; accepted 4 September 2004

Communicated by J. Sherwood

Available online 8 October 2004

Abstract

The interaction of dissolved zinc with calcite {10.4} surfaces during growth and dissolution has been studied using in situ atomic force microscopy and batch sorption experiments.

In situ observations show that the growth of calcite in the presence of zinc occurs by two-dimensional nucleation, the growth rate decreasing with the development of each subsequent layer.

During the dissolution of calcite in the presence of Zn, the pre-existing rhombic-shaped etch pits (formed in pure water) change their morphology to become approximately triangular. Batch-sorption experiments revealed that the dissolution of calcite is coupled with the heterogeneous nucleation of a zinc-bearing precipitate.

© 2004 Elsevier B.V. All rights reserved.

PACS: 61.16.C; 61.72.S

Keywords: A1. Atomic force microscopy; A1: Impurities; A2. Growth from solution; B1: Calcite; B1: Minerals

1. Introduction

The interaction of calcite with several dissolved metals is significant, leading to sorption processes

such as precipitation/coprecipitation, adsorption, and ionic substitution. These processes are coupled with the dissolution of the calcite surface and have geochemical and environmental implications through affecting metal mobility and calcite structure (e.g. Refs. [1–3]). The interaction of metals with minerals is controlled by several variables such as kinetic factors affecting metal cation partitioning between the mineral and

*Corresponding author. Centre for Fuels and Energy, Curtin University of Technology, GPO Box U1987, Perth, WA 6845, Australia. Tel.: +61 8 92661137; fax: +61 8 92661138.

E-mail address: S.Freij@curtin.edu.au (S.J. Freij).

aqueous solution [4], crystal growth rates (e.g. Refs. [5,6]) and the mineral surface structure. The role of calcite surface structure in metal sorption is significant and has been investigated by several studies (e.g. Refs. [1,7,8]). Studies by Paquette and Reeder [1] and Reeder [7] have shown that the incorporation of different ions on growth steps with different crystallographic orientations depends on their ionic radius.

Zinc is a phytotoxic element [9] present in rocks and soil and it affects the plant growth. Anthropogenic sources of zinc in the soil include sewage sludge, compost, agrochemicals, and mine tailings [10].

Various studies have tackled the interaction of zinc with calcite using kinetic/spectroscopic techniques. Glasner et al. [11] reported that the presence of large amounts of zinc in a Ca^{2+} , CO_3^{2-} —bearing fluid, hinders the crystallisation of calcite and favours the formation of hydrozincite. Kinetic studies (e.g. Refs. [12,13]) of the growth of calcite in the presence of zinc reported reduction in the growth rate. Temmam et al. [14] studied the effect of zinc on calcite growth. They found that the strong adsorbing behaviour of zinc decreased the growth rate, increased the surface roughness and triggered the nucleation along macrosteps. Wada et al. [15] reported that the presence of zinc cation during the growth of calcium carbonate in gel favours the formation of aragonite.

Zachara et al. [16] studied the sorption of zinc to calcite surface and suggested that it occurs via exchange with calcium in a surface-adsorbed layer. Cheng et al. [17] studied the interaction of zinc with calcite surfaces using spectroscopy techniques (X-ray standing wave and surface-extended X-ray absorption fine structure) and concluded that Zn^{2+} substitutes for Ca^{2+} in the surface layer. Another spectroscopy study by Reeder et al. [18] of synthetic and natural calcite samples containing traces of Zn confirmed the substitution of Zn^{2+} for Ca^{2+} in octahedral coordination.

A study by Garcia-Sanchez and Alvarez-Ayuso [19] concluded that the sorption of zinc on calcite can be described best by Langmuir model and it occurs by precipitation as hydrozincite ($\text{Zn}_5(\text{OH})_6 \cdot (\text{CO}_3)_2$). El-Korashy [20] studied the sorption of zinc to calcite surfaces and

suggested that it occurs mainly via crystallization of ZnCO_3 .

All these studies provided significant information on the interaction of zinc with calcite at different experimental conditions, using various techniques, but none dealt with the in situ interaction of zinc at the microscopic level, which is necessary to clarify, in order to understand the mechanism of interaction. The objective of this study is to investigate the interaction of zinc with a calcite cleavage surface in undersaturated and supersaturated solutions at the microscopic and macroscopic levels. In situ AFM-growth experiments show that growth occurs by two-dimensional nucleation and the growth rate decreases with the development of each subsequent layer.

In situ AFM-dissolution experiments illustrate the change in etch pit morphology and the heterogeneous nucleation of a zinc-bearing precipitate and these results are correlated with the results of our macroscopic sorption experiments which show that the dissolution of calcite is coupled with the precipitation of hydrozincite.

2. Experimental procedure

2.1. In situ AFM observations

In situ experiments were conducted using a Digital Instruments Nanoscope 111a Scanning Probe Microscope, equipped with a fluid cell, and working in contact mode at 25 °C. Freshly cleaved {10.4} calcite crystals (Iceland spar grade) were used as substrates. At the beginning of every experiment, deionized water was passed over the substrate to adjust the imaging parameters and to remove any attached particles.

For the growth experiment, aqueous solution was prepared by mixing Na_2CO_3 , CaCl_2 , and ZnCl_2 aqueous solutions (final concentrations are: 0.44 mM CaCl_2 , 0.34 mM Na_2CO_3 , and 0.01 mM zinc chloride). The solution pH was measured using a WTW Inolab pH meter. The pH meter was calibrated using standard buffer solutions 6.865 and 9.17 (WTW).

Growth solution was passed over the substrate by injecting fresh solution at intervals of about

2 min to promote growth. The activity coefficients for Ca^{2+} , Zn^{2+} , and CO_3^{2-} , and the saturation indices for the solutions with respect to calcite were calculated using PHREEQC [21]. The supersaturation with respect to calcite is 9.5 (expressed as $\beta_{\text{calcite}} = a(\text{Ca}^{2+})a(\text{CO}_3^{2-})/K_{\text{calcite}}$, where a is the ion activity and $K_{\text{calcite}} = 10^{-8.48}$ is the solubility product. The supersaturation with respect to zinc hydroxide is 2.34 and the supersaturation with respect to zinc carbonate is negligible (0.004). Fluids compositions in the calculations were not equilibrated with respect to atmospheric CO_2 . For the growth studies, approximate step advancement rates were estimated along [010] direction by measuring the dimension of the nuclei in this direction in the image sequence.

For the dissolution study, 10^{-2} M zinc chloride solution was prepared, with a pH of 3. After passing deionized water and establishing the crystallographic directions of the substrate, the entire volume of the fluid cell was exchanged five times and the dissolution process was imaged in this standing solution over a period of 1–2 h.

2.2. Batch-sorption experiments

Powdered calcite crystals (particle-sizes 100–200 μm and $<100 \mu\text{m}$) were obtained by crushing calcite crystals (Iceland spar Grade) using an agate mortar and sieving the produced grains using Retsch standard analytical sieves.

Sorption experiments were carried out at room temperature and at atmospheric P_{CO_2} by reacting the solids with aqueous solutions of ZnCl_2 (Zn concentration ranges from 50 to 500 mg/L which is equivalent to 0.76–7.6 mM, and initial pH of solutions ranges from 3.8 to 4.6) in a continuously stirred 50 mL PPN tubes (Greiner Bio-One). The solid/liquid ratio was 2 g/L. The time to which the sorption rate is negligible was ~ 72 h, based on preliminary kinetic experiments in which the most concentrated Zn solution was used. The interacted calcite samples were separated from the suspensions using Nalgene filtration apparatus with Millipore 0.45 μm membrane filters, and air-dried. The filtrates were analysed for Ca^{2+} and Zn^{2+} using ICP–AES (Thermo Jarrell Ash, Atom Scan 25), and the solids were studied by SEM–EDS

(Jeol JSM-6300F equipped with a Link EDS) and powder-XRD (Philips X'Pert diffractometer, $\text{CuK}\alpha$ -radiation).

3. Results

3.1. The interaction of zinc with calcite during growth

Before presenting our experimental observations, we briefly explain the surface structure of calcite.

The structure of the {10.4} cleavage faces can be described based on the periodic bond chain (PBC) model of Hartman and Perdok [22]. These faces contain three non-equivalent PBC's parallel to the $\langle\bar{4}41\rangle$, $\langle 2\bar{2}1\rangle$, and $\langle 010\rangle$ directions. Steps parallel to a given set of PBCs are structurally identical, but because of the orientation of such steps to the symmetry elements, opposite directions of advancement for a given steps are non-equivalent ($[\bar{4}41]_+$, $[48\bar{1}]_+$, $[\bar{4}41]_-$ and $[48\bar{1}]_-$, according to the notation used by Staudt and Reeder [23]. Fig. 1 shows typical rhombic water-induced etch pits on

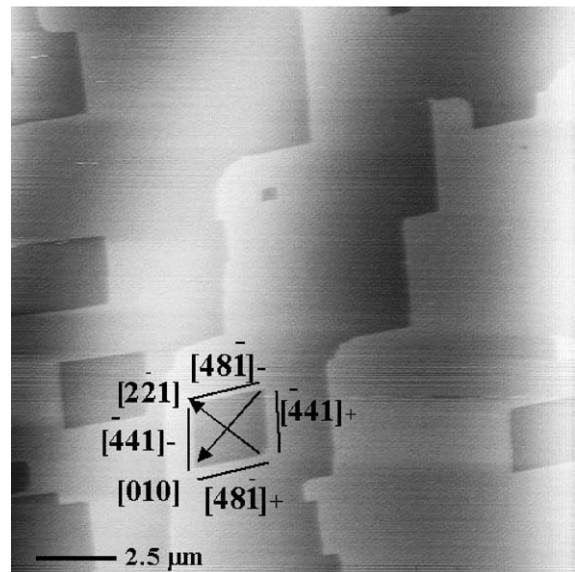


Fig. 1. AFM image of calcite surface in water, showing the typical rhombohedral etch pits, with the crystallographic directions indicated.

a calcite $\{10.4\}$ surface, defined by the $[\bar{4}41]$ and $[48\bar{1}]_+$ steps.

The $[\bar{4}41]_+$ and $[48\bar{1}]_+$ steps define the relatively large kinks (obtuse corner) and the $[\bar{4}41]_-$

and $[48\bar{1}]_-$ steps define the relatively constrained and smaller kinks (acute corner). The $[\bar{4}41]_+$ and $[48\bar{1}]_+$ steps retreat faster than the $[\bar{4}41]_-$ and $[48\bar{1}]_-$ steps during dissolution. Therefore,

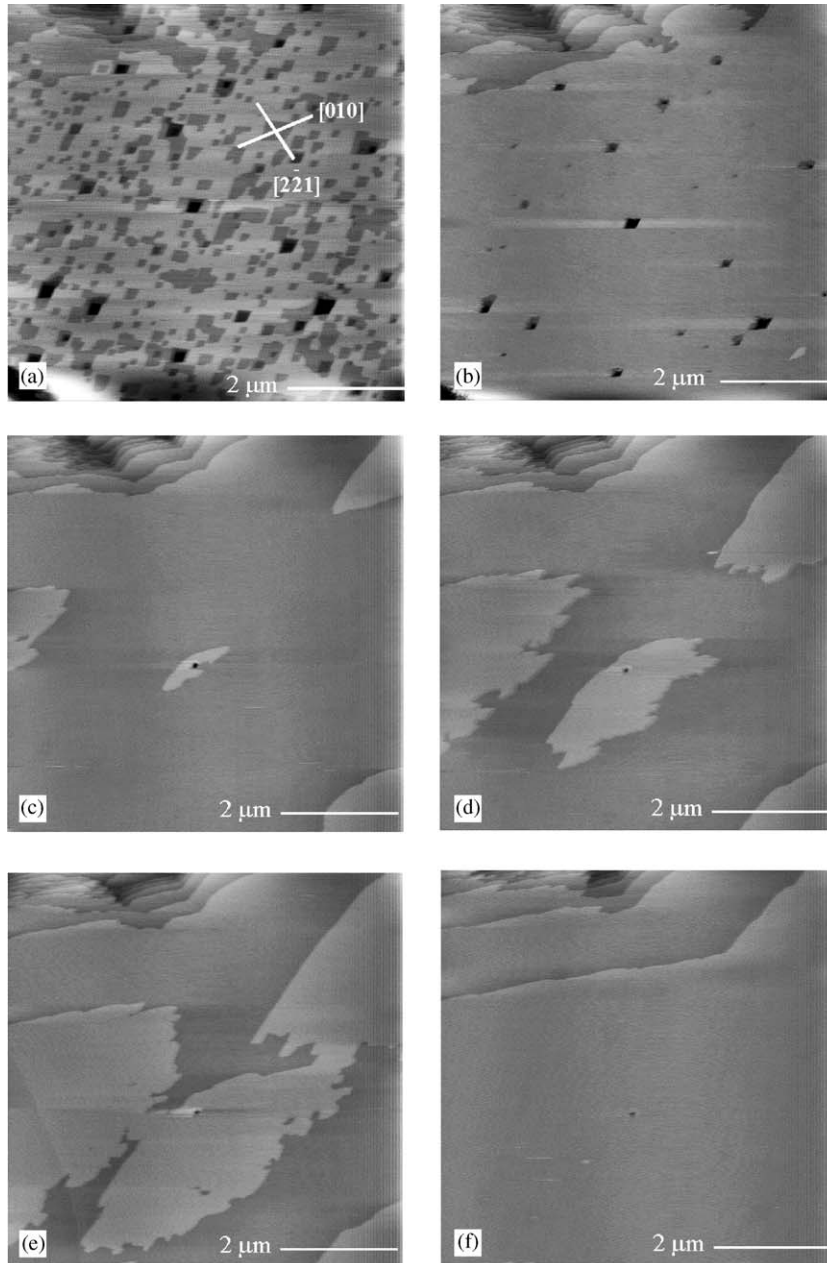


Fig. 2. An in situ growth sequence on calcite $\{10.4\}$ surface in solution. (a) $t = 0$, (b) $t = 4$ min, (c) $t = 28$ min, (d) $t = 40$ min, (e) $t = 50$ min, (f) $t = 76$ min.

by direct observation of the etch-pits expansion it is possible to determine the crystallographic directions on calcite surfaces prior to every experiment.

Fig. 2a shows the surface of a calcite crystal a few minutes after dissolution in deionized water, a flat area with shallow etch pits (0.3 nm in depth) and several deep etch pits. Figs. 2b–e show a

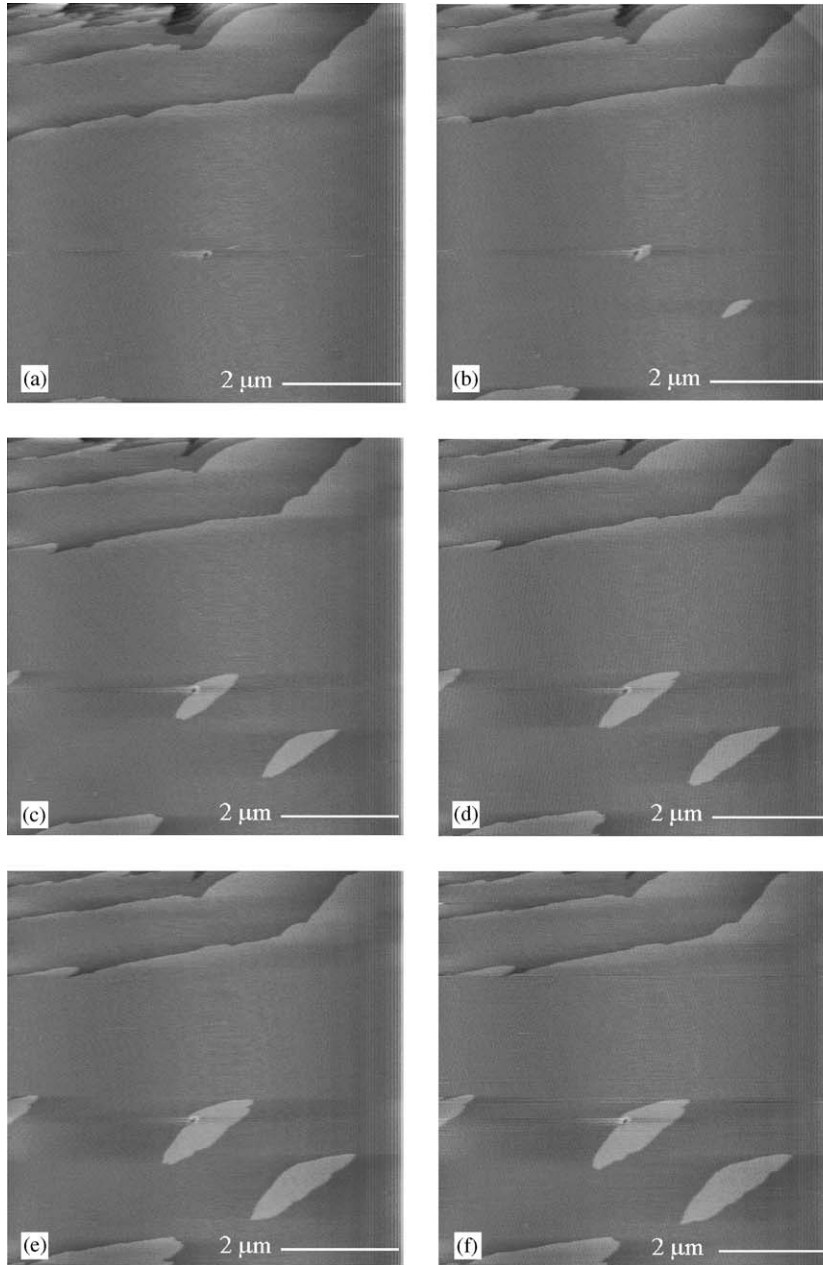


Fig. 3. An in situ growth sequence on calcite {10.4} surface in solution. (a) $t = 99$ min, (b) $t = 107$ min, (c) $t = 121$ min, (d) $t = 125$ min, (e) $t = 129$ min, (f) $t = 133$ min.

sequence of images taken of the surface of calcite after growth in solution. The supersaturation with respect to zinc hydroxide is 2.34 and the supersaturation with respect to zinc carbonate is negligible (0.004)

Initial growth in solution (4 min) leads to filling of shallow etch pits, spreading of monomolecular steps and formation of elongated two-dimensional nuclei on flat areas of the surface (Fig. 2b). The height of the nuclei is 0.3 nm and they grow mainly in the [0 1 0] direction developing irregular edges (Fig. 2c). With further growth (Figs. 2d–e), the nuclei spread and coalesce leading to the formation of one whole layer. The step advancement rate is 3.2 nm/s in the [0 1 0] direction and 1.3 nm/s in the [2 $\bar{2}$ 1] direction. The irregularity of the nuclei edges suggests that zinc is incorporated in this growth layer which therefore has a new composition given by the general formula $\text{Ca}_x\text{Zn}_{1-x}\text{CO}_3$.

Fig. 3 illustrates a second-layer growth on the surface of the same crystal, which starts after approximately 23 min from the formation of whole layer (Fig. 2f). This shows that the first formed layer exhibit an inhibiting effect on the growth of subsequent layers.

Fig. 3a shows the beginning of two-dimensional nucleation at exactly the same position (etch pit) where a nucleus was formed during the first-layer growth. This may indicate that the surface structure has control on the sites of two-dimensional nucleation.

Fig. 3b shows the formation of another two nuclei. Further spreading of the nuclei in the [0 1 0] direction is shown in Figs. 3c–f. The growth proceeds slower and the step advancement rate is 1.2 nm/s in [0 1 0] direction and 0.3 nm/s in the [2 $\bar{2}$ 1] direction.

Fig. 4 shows the same surface 2 min after passing deionized water over it. Dissolution occurs mainly by formation of few deep etch pits and some shallow ones, almost at the same position as in the initial dissolution of the surface (Fig. 2a), before the beginning of the experiment. This may indicate that some of these etch pits are formed at sites of dislocations. The nuclei almost still have the same length, and the step edges are at the same position, suggesting that the solubility of the newly formed layers is lower than the solubility of calcite.

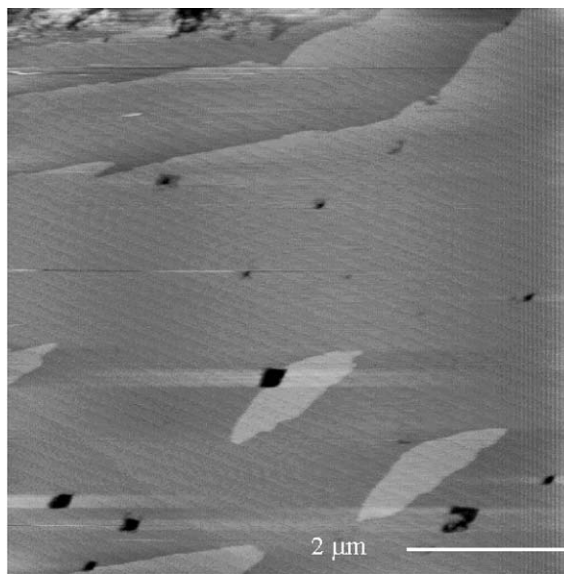


Fig. 4. An AFM image showing the surface of calcite (area in Fig. 3) ca. 2 min after flowing deionized water.

Alternatively, the presence of zinc in these layers does not introduce defects where etch pits can rapidly nucleate, this may suggest that calcite and the overgrowth have similar structure.

3.2. The interaction of zinc with calcite during dissolution

In situ dissolution experiments were conducted in 10^{-2} M ZnCl_2 solution with a pH of 3. This solution is undersaturated with respect to calcite or any Zn phase (carbonate, hydroxide). The dissolution process is very fast and considerable precipitation occurs directly after exchanging the volume of the fluid cell with ZnCl_2 solution, which makes imaging difficult. Fig. 5a shows the original crystal surface, few minutes after dissolution in deionised water. Fig. 5b represents the crystal surface after 11 min in ZnCl_2 solution. Fast dissolution occurs and new etch pits are formed with an almost triangular shape. This is possibly due to the sorption of zinc at the obtuse kink. No precipitation is observed in the scanned area. However, when a larger area is imaged outside that scanned area (Fig. 5c, 22 min from the beginning of the experiment), thick particles

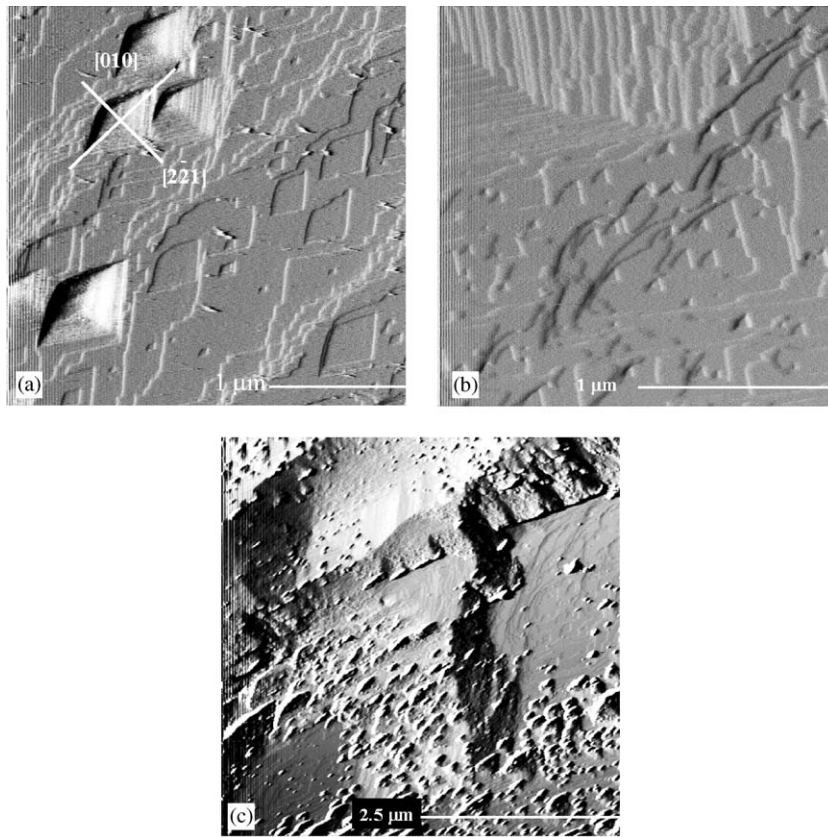


Fig. 5. AFM images showing dissolution of calcite. (a) In pure water, (b) 11 min in 10^{-2} M ZnCl_2 solution, (c) 22 min in 10^{-2} M ZnCl_2 solution.

(height more than 10 nm) have formed on the surface, possibly by heterogeneous nucleation of a Zn-bearing phase. This shows that the interaction between the AFM tip and the calcite surface (in contact mode AFM) can cause particle stripping from the surface during the course of dissolution/precipitation experiments.

3.3. Batch-sorption experiments

Our macroscopic batch-sorption experiments show that the removal of Zn from initially undersaturated aqueous solutions is fast and considerable. In the case of the coarser calcite (100–200 μm) the metal uptake is found to be in the range 23–172 mg/g (71–99% removal), whereas in the case of the fine calcite (<100 μm) it is even

higher (metal uptake 23–210 mg/g, and removal 87–99%). However, the evaluation of the sorption data indicates that the selectivity of powdered calcite for Zn is higher at lower metal concentrations. This is illustrated by the sorption distribution coefficients K_d ($K_d = C_s/C_w$, where C_s is the concentration in the solid and C_w is the concentration in the aqueous solution) which describes the distribution of the metal ions between the carbonate solid and solution independently from the mass of the solid (Fig. 6a).

At the very beginning of the experiments the aqueous solutions are very virtually free of calcium, but the calcium concentration increases as calcite dissolves. It is also evident that the sorption of Zn (through several mechanisms such as adsorption, possible absorption, and mainly

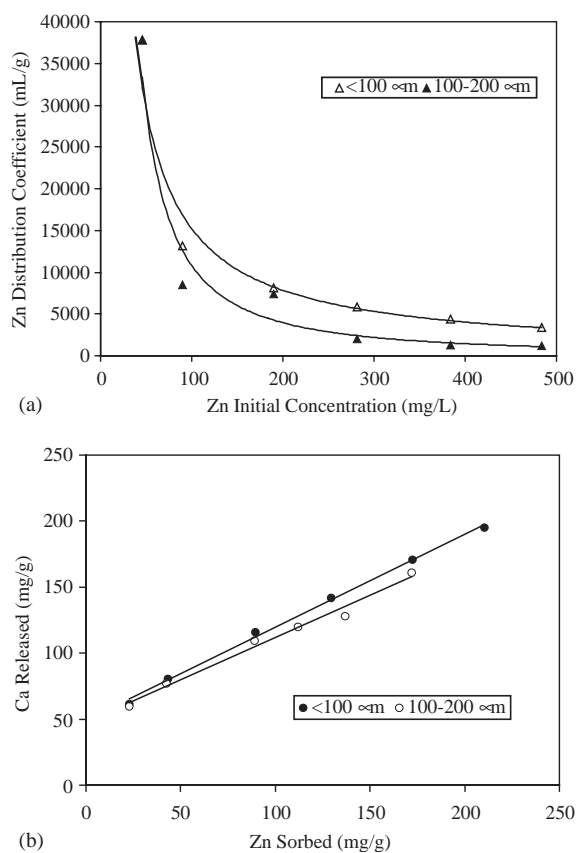


Fig. 6. Macroscopic data from ICP–OES analyses concerning the interaction of powdered calcite crystals (particle-size: < 100 and 100–200 μm) with Zn aqueous solutions (initial concentration range: 50–500 mg/L) at room temperature and atmospheric P_{CO_2} .

surface precipitation/co-precipitation) and the dissolution of the calcite surfaces (expressed by the Ca release) are coupled chemical processes and entirely correlated until the establishment of the apparent equilibrium (Fig. 6b). Consequently, the pH of the solutions increases with the dissolution, in the range 6.9–7.8. SEM–EDS studies of the interacted calcite grains, demonstrate that massive surface precipitation takes place leading to overgrowth of Zn-containing solid phases. They appear in the form of distinct small aggregates, covering a major part of the dissolved calcite surfaces (Fig. 7a). This is in agreement with our in situ AFM observations, which shows precipitation

of discrete particles. Detailed powder-XRD study of calcite solids (Fig. 7b) shows that the aforementioned Zn-containing phases are predominantly zinc hydroxycarbonates (hydrozincite $(\text{Zn}_5(\text{CO}_3)_2(\text{OH})_6)$, card # 19-1458[®] 2000 JCPDS), in addition to minor composite phases corresponding to the rare mineral minrecordite $(\text{CaZn}(\text{CO}_3)_2)$, card # 35-667[®] 2000 JCPDS). The formation of smithsonite (ZnCO_3) , card # 8-449[®] 2000 JCPDS) or of any other Zn anhydrous carbonate is not observed.

4. Discussion

Our AFM-growth experiments show that the growth of calcite in the presence of zinc proceeds with two-dimensional nucleation and the growth rate decreases further with each subsequent layer.

This is in agreement with the findings of Temmam et al. [14] who studied the effect of zinc on calcite growth. They found that the strong adsorbing behaviour of zinc decreased the growth rate, increased the surface roughness and triggered the nucleation along macrosteps.

The growth of calcite in the presence of zinc is highly anisotropic in the [0 1 0] direction, which is unlike the growth of calcite in the presence of cobalt that yields almost isotropic nuclei, exhibiting similar step advancement rates in [0 1 0] and [2 2 1] directions [24].

The growth of the second layer in this study is slower than growth of first layer, although the supersaturation of the solution in the presence of zinc with respect to a possible intermediate solid solution composition will increase [24]. This is similar to our observations in the presence of cobalt [25]. In the latter study, we referred to a model proposed by Astilleros et al. [26], who suggested a model for the layer-by-layer growth of solid solutions, which takes into account the strain induced by the formation of a solid solution. Within the first layer of growth which has a new composition given by the general formula $\text{Ca}_x\text{M}_{1-x}\text{CO}_3$, the distribution of foreign cations may be random so growth proceeds as growth in pure solution. With further growth on the newly formed surface, relaxation of the strain perpendi-

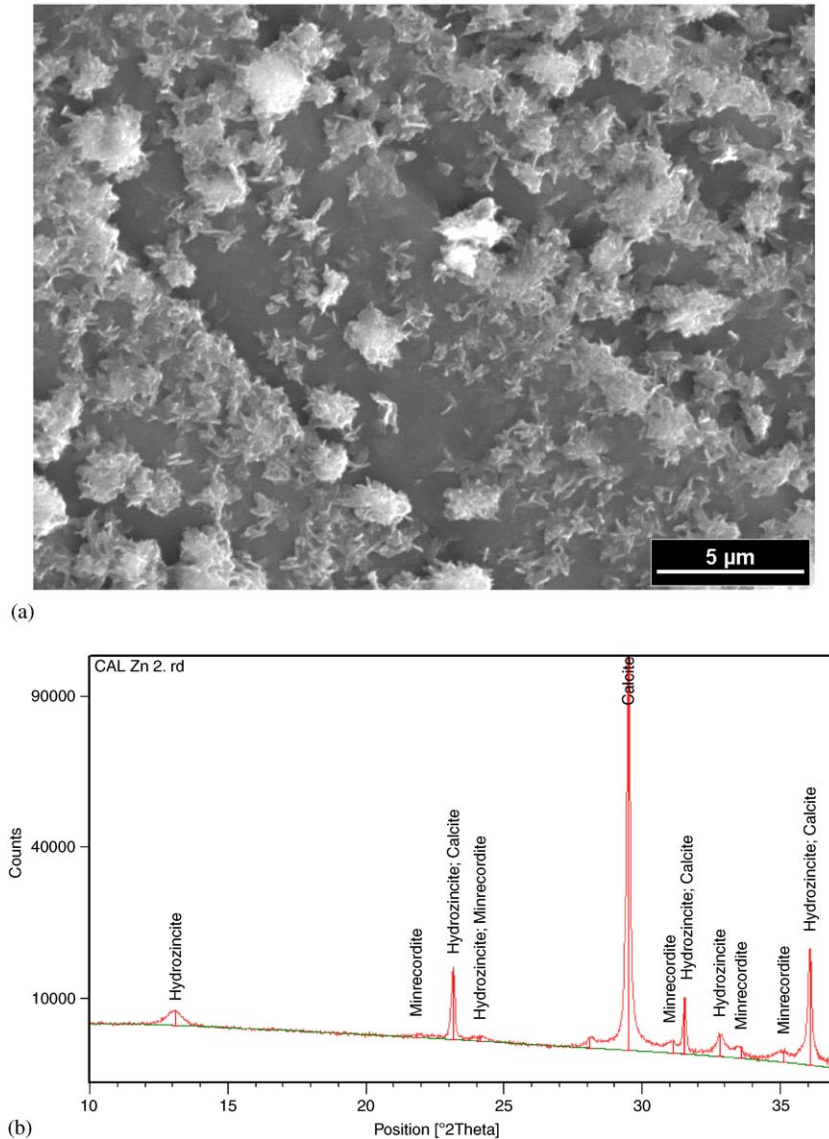


Fig. 7. SEM image and powder-XRD data demonstrating the overgrowth of zinc containing crystal aggregates (mean diameter $\sim 2\mu\text{m}$) on the dissolved surface of a calcite grain from interacted powdered sample.

cular to the layer will introduce local variations in the bond length and consequently change of surface topography. This leads to the decrease in growth rates and change in growth mechanism. In the current study, we did not observe a clear reproduction of the original surface topography as a result of the inhibiting effect of foreign cation

during growth on the newly formed surface, as reported in previous studies [25,26]. This could be related to the surface topography of the surface prior to growth.

The difference in nuclei shape formed in the presence of cobalt and in the presence of zinc suggests that zinc and cobalt have different step-

specific preference, although they have similar ionic radius (both smaller than calcium). This is in agreement with Reeder [7] who has shown that zinc exhibits step-specific preferences similar to those of ions larger than calcium (such as Ba and Sr). According to Paquette and Reeder [1] and Reeder [7], these ions are enriched in the $[441]_+$ and $[481]_+$ steps, which define the relatively large kinks (obtuse kink), during coprecipitation experiments of calcite.

Also the difference in the interaction of cobalt and zinc with calcite, can be partially related to the higher solubility of zinc in calcite, compared to cobalt [27].

The shape of the nuclei formed in the presence of zinc is similar to the shape of the nuclei reported by Astilleros et al. [28] during the growth of calcite in the presence of barium.

Dissolution of calcite in $ZnCl_2$ solution changes the morphology of the etch pits from rhombic to semi triangular. This is similar to the observation of Godelitsas et al. [3] who studied the interaction of Hg^{2+} (an ion slightly larger than Ca^{2+}) with calcite surfaces. Heterogeneous nucleation of a zinc phase is observed in the AFM and SEM images of calcite surfaces dissolving in $ZnCl_2$ solution.

Our macroscopic batch sorption experiments reveal that the removal of Zn from aqueous solutions is fast and considerable. The dissolution of calcite is coupled with the heterogeneous nucleation of zinc containing precipitate. These processes involve the release of Ca^{2+} and CO_3^{2-} from calcite surfaces to the fluid and the subsequent reaction between the ions in solution and the foreign metal cation (Zn^{2+}). For our experimental conditions, this produces mainly hydrozincite crystals, in addition to minor composite phases corresponding to the rare mineral minrecordite ($CaZn(CO_3)_2$).

Acknowledgements

S.J. Freij acknowledges the receipt of Humboldt Research Fellowship from the Alexander von Humboldt Foundation.

We would like to thank the European Commission for support within the frames of the European Research Training Network on “Quantifying Dissolution and Precipitation of Solid-Solutions in Natural and Industrial Processes” (contract HPRN-CT-2000-00058) as well as DFG (Deutsche Forschungsgemeinschaft) for support of the AFM laboratory.

References

- [1] J. Paquette, R.J. Reeder, *Geochim. Cosmochim. Acta* 59 (1995) 735.
- [2] J.D. Rimstidt, A. Balog, J. Webb, *Geochim. Cosmochim. Acta* 62 (1998) 1851.
- [3] A. Godelitsas, J.M. Astilleros, K. Hallam, J. Löns, A. Putnis, *Miner. Mag.* 67 (2003) 1193.
- [4] J.W. Morse, M.L. Bender, *Chem. Geol.* 82 (1990) 265.
- [5] R.B. Lorenz, *Geochim. Cosmochim. Acta* 45 (1981) 553.
- [6] A. Mucci, J.W. Morse, *Geochim. Cosmochim. Acta* 47 (1983) 213.
- [7] R.J. Reeder, *Geochim. Cosmochim. Acta* 60 (1996) 1543.
- [8] E.J. Elzinga, R.J. Reeder, *Geochim. Cosmochim. Acta* 66 (2002) 3943.
- [9] I. Montilla, M.A. Parra, J. Torrent, *Plant and Soil* 257 (2003) 227.
- [10] L. Kiekens, Zinc, in: B.J. Alloway (Ed.), *Heavy Metals in Soils*, second ed., Blackie Academic and Professional, Glasgow, 1990, pp. 284–305.
- [11] A. Glasner, D. Weiss, *J. Inorg. Nucl. Chem.* 42 (1980) 655.
- [12] H.J. Meyer, *J. Crystal Growth* 66 (1984) 639.
- [13] A. Gutjahr, H. Dabringhaus, R. Lacmann, *J. Crystal Growth* 158 (1996) 310.
- [14] M. Temmam, J. Paquette, H. Vali, *Geochim. Cosmochim. Acta* 64 (2000) 2417.
- [15] N. Wada, K. Yamashita, T. Umegaki, *J. Crystal Growth* 148 (1995) 297.
- [16] J.M. Zachara, J.A. Kittrick, J.B. Harsh, *Geochim. Cosmochim. Acta* 52 (1988) 2281.
- [17] L. Cheng, N.C. Sturchio, J.C. Woicik, K.M. Kemner, P.F. Lyman, M.J. Bedzyk, *Surf. Sci.* 415 (1998) L976.
- [18] R.J. Reeder, G.M. Lamble, P.A. Northrup, *Am. Miner.* 84 (1999) 1049.
- [19] A. Garcia-Sanchez, E. Alvarez-Ayuso, *Miner. Eng.* 15 (2002) 539.
- [20] S.A. El-Korashy, *J. Mater. Sci.* 38 (2003) 1709.
- [21] D.L. Parkhurst, C.A.J. Appelo, 2000. Users guide to PHREEQC (Version 2). A computer program for speciation, batch-reaction, one-dimensional transport, and inverse geochemical calculations, US Geological Survey Water-resources Investigations Report 99-4259, p. 311.
- [22] P. Hartman, W.G. Perdok, *Acta Crystallogr.* 8 (1955) 521.

- [23] W.J. Staudt, R.J. Reeder, *Geochim. Cosmochim. Acta* 58 (1994) 2087.
- [24] J.M. Astilleros, C.M. Pina, L.A. Fernandez-Diaz, A. Putnis, *Geochim. Cosmochim. Acta* 67 (2003) 1601.
- [25] S.J. Freij, A. Putnis, J.M. Astilleros, *J. Crystal Growth* 267 (2004) 288.
- [26] J.M. Astilleros, C.M. Pina, L. Fernandez-Diaz, A. Putnis, *Surf. Sci.* 545 (2003) 767.
- [27] J.R. Goldsmith, in: *Reviews in Mineralogy*, American Society of America, Washington, 1990, p. 65.
- [28] J.M. Astilleros, C.M. Pina, L.A. Fernandez-Diaz, A. Putnis, *Geochim. Cosmochim. Acta* 64 (2000) 2965.